J. Membrane Biol. 208, 91–102 (2005)
DOI: 10.1007/s00232-005-0822-z

The Journal of
Membrane
Biology



# Nano to Micro — Fluorescence Measurements of Electric Fields in Molecules and Genetically Specified Neurons

**R. Blunck, B. Chanda, F. Bezanilla**
Departments of Physiology and Anesthesiology, David Geffen School of Medicine at the University of California, Los Angeles, California

Received: 12 December 2005

**Abstract.** Our central nervous system is based on the generation and propagation of electrical signals along the neuronal pathways. These variations of the membrane potential are arranged by the concerted action of ion channels in the neuronal membrane. Therefore, the exact measurement of the electric field in the central nervous system is the focus of intensive investigation. While electrophysiological methods provide exact measurements on the single-cell or single-molecule level with high temporal resolution, they are limited in their spatial resolution ranging from a few single cells to a single molecule. To thoroughly understand how the voltage-dependent ion channels sense the membrane potential and are precisely gated by it, the electric field within the protein has to be investigated. Likewise, the propagation of electrical impulses in a network of neurons involves a large number of cells, which have to be monitored simultaneously. For these endeavors, optical methods have proven to be useful due to their scalability, temporal and spatial resolution. Here, we will summarize the properties of the optical probes that we used to determine the electrical field strength within voltage-sensitive ion channels and discuss the hybrid approach to detect membrane potential changes in genetically specified neurons in terms of design, limitations and future developments.

**Key words:** Voltage-gated ion channel — Fluorescence — Potentiometric dye — ANEPIA — Hybrid voltage sensor — hVOS — GFP — Farnesyl — Dipicrylamine

## Introduction

The central nervous system (CNS) uses electrical signaling for communication and processing of information. These signals are manifested as rapid voltage changes across the membrane as a result of the activity of ligand-gated and voltage-gated ion channels. Therefore, the understanding of generation and processing of information in the CNS requires the measurement of voltage changes with high accuracy. The dominant technique has been the use of microelectrode-based methods that can measure membrane potential changes with extremely high temporal resolution and high sensitivity. Variations of these techniques enabled the measurement of the activity at the level of a single ion channel. Nevertheless, microelectrode-based methods have the significant drawback of limited spatial resolution. They provide averaged information about voltage changes over the whole cell when recording intracellularly and over groups of cells in an extracellular configuration. Electric field potentials in biological systems tend to be rather inhomogeneous. For instance, in the nerve cells action potentials are typically initiated in the axon hillock and the resultant voltage pulse travels down the axon to the nerve terminal. These spatial inhomogeneities in the electric field are not just limited to different morphologically distinct regions of the tissue or in the neuron but also extend to nanoscale crevices of molecular dimensions within the plasma membrane proteins that reside in these excitable cells. Measurements of electric field by optical methods, particularly those based on fluorescent probes, are capable of following potential changes with both high time and spatial resolution.

Optical measurements of electric field changes in biological systems were brought into perspective in the early 1970s by Cohen, Salzberg and colleagues when they surveyed hundreds of different probes as

*Current address for F.B.:* Institute for Molecular Pediatrics Science, The University of Chicago, CIS Building, Room W224, 929 East 57th Street, Chicago, IL 60637, USA
*Correspondence to:* F. Bezanilla; email: FBezanilla@UChicago.edu

membrane potential indicators (reviewed in Cohen & Salzberg, 1978). Since then, fluorescent probes of membrane potential have been used to measure simultaneous activity of populations of neurons and to follow waves of electrical impulses within the neurons in a variety of tissues. In addition to having high temporal resolution, optical methods are minimally invasive compared to electrode-based methods. Therefore, the number of optical detectors can be scaled up relatively easily (diode array, ECCD cameras). Both of these properties make optical probes almost ideal for monitoring simultaneous activity from groups of neurons.

Nevertheless, the full potential of optical methods to study information processing in neuronal circuits has not been realized due to their lack of specificity and, paradoxically, their inability to stain many regions of interest. A brain-slice preparation contains not only neurons but also a large population of non-excitable cells in their immediate surrounding. Unless the dye is injected into a cell, staining with synthetic membrane potential-sensing probes leads to indiscriminate loading of the dye on membranes from all cells (Konnerth, Obaid & Salzberg, 1987). This significantly increases the fluorescence background, resulting in diminished signal-to-background ratios. Furthermore, many synthetic potential-sensing dyes are also highly hydrophobic so that they are trapped in superficial layers and are unable to stain neurons that are in the deeper layers of the slice. Therefore, much of the recent research on the development of membrane potential probes has focused on designing membrane potential-sensing probes that can be targeted to specific cell types as well as subcellular locations.

Some of the voltage-sensing probes that can be targeted to a cell or even to a specific part of a molecule have shown considerable promise in their ability to measure electric field changes at the cellular level or at the molecular level, respectively. In this last category, probes that measure fields at specific sites on voltage-dependent ion channels have provided useful insights into the physical mechanisms of voltage-gating in potassium channels. In this review, we will discuss the recent advances in development of targeted optical probes that sense changes in electrical potentials both at the level of the plasma membrane and at the intramolecular level. We will also discuss the limitations of the current generation of targeted potential-sensing probes and consider future directions.

## Measurement of the Local Electric Field within a Membrane Protein

Because membrane proteins are structured, their dielectric properties are anisotropic, a property which is expected to reshape the plasma membrane electric field inside the protein. The measurement of these local electric fields at different sites inside the protein molecule has been undertaken only in the case of *Shaker*, a voltage-gated $K^+$ channel. In the next two sections, we have summarized the motivation for, and the results of this study.

### The Voltage Sensor in Ion Channels

Voltage-gated ion channels consist of tetramers ($K^+$ channels) or monomers with four domains ($Na^+$, $Ca^{++}$ channels) each with six transmembrane helices (Fig. 1*A*). The fourth transmembrane helix (S4) in each monomer or domain contains a number of positively charged (+) arginines or lysines separated by hydrophobic residues (x) in a +xx+xx+xx-motif (Noda et al., 1984). Changes in the membrane potential lead to a conformational change of the S4 helix, which results in opening of the ion-conducting pore (Aggarwal & MacKinnon, 1996; Seoh et al., 1996). Site-specific fluorescence measurements of ion channels under voltage-controlled conditions have allowed direct tracking of the conformational change of the voltage sensor in expression systems ranging from oocytes (Mannuzzu, Moronne & Isacoff, 1996; Cha & Bezanilla, 1997; Chanda & Bezanilla, 2002; Schonherr et al., 2002) to cells (Blunck et al., 2004). In this very powerful method, a fluorophore is attached to the SH-group of a cysteine via a thiol-reactive linker and reports local conformational changes. Although 12−13 elementary charges ($e_0$) are moved through the entire electrical field upon opening of a single channel (Aggarwal & MacKinnon, 1996; Seoh et al., 1996), it was found in fluorescence measurements that there are no large transmembrane movements of the S4 helix (Cha et al., 1999; Blunck et al., 2004; Chanda et al., 2005a; Posson et al., 2005). Replacing the 2$^{nd}$, 3$^{rd}$ and 4$^{th}$ charged residues (R365, R368 and R371) by histidine in the Shaker $K^+$ channel revealed that these positions are exposed to the cytosolic and external side in the hyperpolarized and depolarized state, respectively (Fig. 1*B*). The histidine experiments also revealed the existence of a proton pore in the closed state at position R362H (Starace & Bezanilla, 2004) and in the open state at position R371H (Starace & Bezanilla, 2001), indicating that the electric field is concentrated in a small region of the protein. Based on these experimental findings, the "transporter model" was proposed (Fig. 1, Chanda et al., 2005a). In this model, the concentrated field is generated by the conducting medium that penetrates deep into the channel protein via water-filled crevices around the voltage sensor. It is suggested that the transport of 12−13 $e_0$ across the field measured experimentally is achieved by a small tilt of the S4 segment that translocates the charged arginines from an internal water crevice at hyperpolarized potentials to an external crevice at depolarized potentials (Fig. 1*B*, Bezanilla, 2000; Chanda et al.,

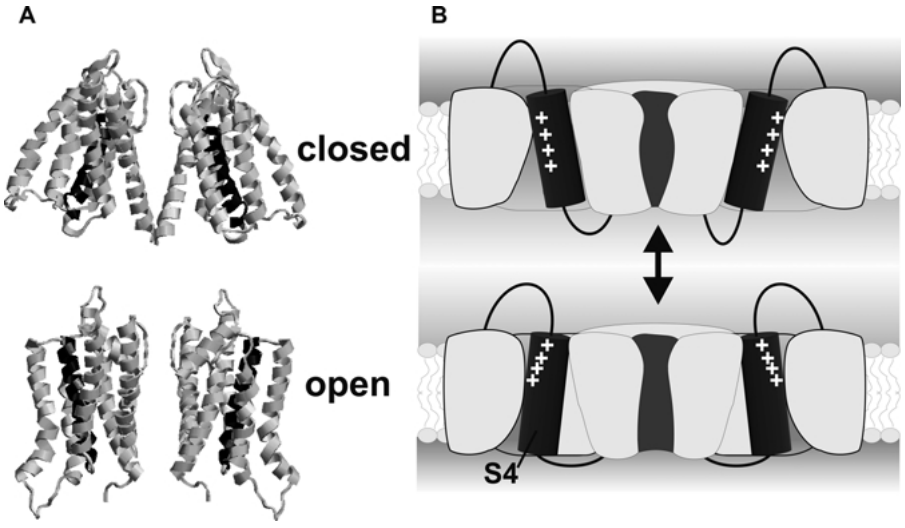


**Fig. 1.** The transporter model. (*A*) Molecular model of the *Shaker* potassium channel (Chanda et al., 2005a) in closed configuration at resting potential (*top*) and open configuration at depolarizing potential (*bottom*). The positively charged helix S4 is shown in dark and the other helices are depicted in light grey. (*B*) Schematic of the transporter model. The voltage-sensing helix S4 (*dark*) is surrounded by water-filled crevices that reach deep into the protein. The electric field is concentrated over a very short distance between the two crevices. As a result of conformational changes in the S4 and the surrounding helices, the water-filled crevices rearrange so that the charges get exposed to the opposite site.

2005a). A key feature of this mechanism is that the electric field around the charged residues of S4 is concentrated by the surrounding protein so that the determination of the electric field with higher resolution at a specified location becomes important. Thus, the use of a voltage-sensitive dye attached at different regions of the protein was used to demonstrate experimentally the inhomogeneity of the electric field within the channel protein.

## Local Electric Field in Voltage-sensitive Ion Channels

The dipole moment of dyes like di-4- and di-8-ANEPPS (Zhang et al., 1998) interacts with the electric field (Stark effect) so that the excitation and emission spectra are shifted proportionally to the electric field. This wavelength shift in excitation and emission spectra is also referred to as the electrochromic shift. By choosing a particular combination of excitation and emission interference filters, these shifts can be translated into intensity changes. Leslie Loew and his colleagues attached thiol-reactive maleimide (di-1-ANEPMI) or an iodoacetemide (di-1-ANEPIA) to one end of the ANEP chromophore (Fig. 2*A*; Asamoah et al., 2003)[1]. By introducing cysteine residues in specified locations of the channel protein, it is possible to attach these dyes at predetermined sites and thus report local changes in the electrical field strength. Di-1-ANEPIA, compared with di-1-ANEPMI, had much less nonspecific background labeling and was therefore better suited for use in oocytes. Single cysteine mutants of the *Shaker* $K^+$ channel were expressed in *Xenopus* oocytes and fluorescence detected from cut-open oocytes under voltage-clamp conditions (Cha & Bezanilla, 1998). The response of di-1-ANEPIA to depolarizing voltage pulses consisted of two main components (Fig. 2*B*): with the voltage pulse, a very fast change in the fluorescence signal was observed that had the time course of the charging of the membrane capacitance. This fast component was followed by a slow component that correlated roughly with the gating charge movement (Asamoah et al., 2003). Upon return to the resting potential (−90 mV), an extremely fast and a slow component are again observed. The very fast responses are the actual electrochromic signals of the ANEP chromophore. This process is extremely fast, since it is an interaction of the electronic state of the dye molecule with the electric field strength, and in this case its speed is limited by the charging time of the membrane capacitance by the voltage-clamp circuitry. The amplitude of the fast components ($E_{ON}$ and $E_{OFF}$) reflect the electric field changes in response to the voltage pulse. The slower component, on the other hand, correlates with the gating charge movement, indicating that it is caused by the conformational change the S4 undergoes upon depolarization. The

[1]di-1-ANEPMI: 1-[3-(ß-Maleimidopropionyl) aminopropyl]-4-[ß-[2-(dimethylamino)-6-naphtyl] vinyl] pyridinium bromide; di-1-ANEPIA: 1-[3-(Iodoacetyl) aminopropyl]-4-[ß-[2-(dimethylamino)-6-naphtyl] vinyl] pyridinium bromide.

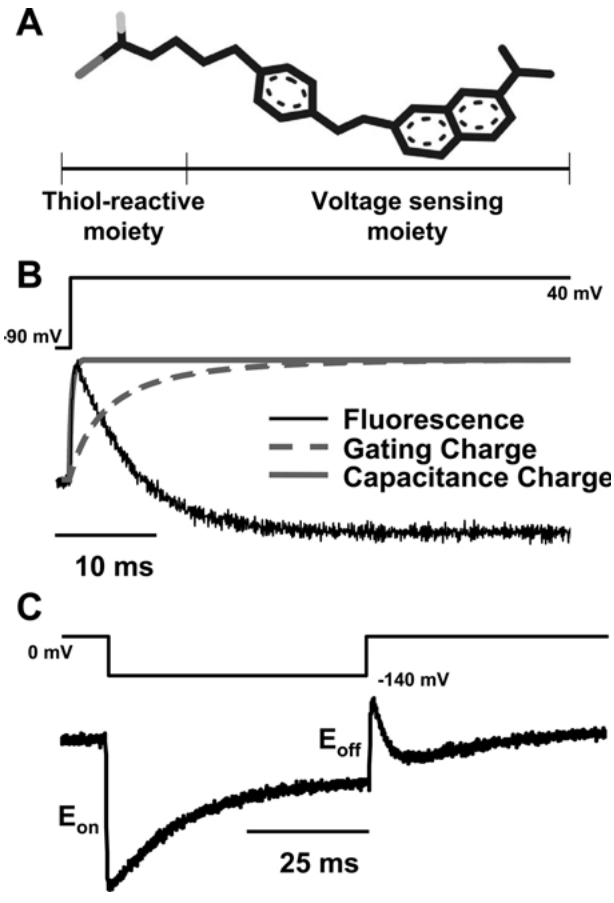


**Fig. 2.** Di-l-ANEPIA. (*A*) Structure of di-1-ANEPIA: l-[3-(Iodoacetyl) aminopropyl]-4-[β-[2-(dimethylamino)-6-naphtyl] vinyl] pyridinium bromide (Asamoah et al., 2003). (*B*) Fluorescence signal of di-1-ANEPIA attached to 354C expressed in *Xenopus* oocytes. The signal (*black trace*) comprises the fast electrochromic signal — following the capacitive charge (*grey*, *solid*) — and the slower fluorescence change caused by the subsequent conformational change in the voltage sensor (*grey*, *dashed*) as the gating charge time course. (*C*) $E_{ON}$ and $E_{OFF}$ of the signal are not symmetric, since the electric field in resting and activated configuration of the voltage sensor is different.

conformational change of the S4 and a reorientation of the water-filled crevices around it cause the electric field to alter its position and strength so that the di-1-ANEPIA fluorescence is changed. At the end of the pulse, upon returning to the resting potential, the OFF signal ($E_{OFF}$) is not symmetric with the ON signal ($E_{ON}$), since the electric field strength of the specified position at hyperpolarized potential is measured. In Fig. 2*C*, $E_{ON}$ reflects the field strength at 0 mV, $E_{OFF}$ at −140 mV.

Scanning the residues where the probe was attached along the extracellular part of the channel and into the S4 helix (345−365) reveals the profile of the electric field around the voltage sensor. The field progressively increases towards the center of the helix and reaches its peak at position 365 (Fig. 3*A*). This profile is in accordance to the transporter model postulating the existence of water-filled crevices. Within the crevices the electric field lines are compressed so that the field strength increases at positions further down the crevice (Fig. 3*B*). In particular, in the neighborhood of the proton pore R362H (Starace & Bezanilla, 2004), the field is concentrated in the small bridge between the outside and the internal crevice.

An alternative, less quantitative approach to probing the electric field strength around S4 uses tethered charges attached to a single position within the S4 (R362C) with linkers of variable length (Ahern & Horn, 2005). The charge is then located at different positions within the field and this influences the gating properties of the channel.

The scanning of electric field strength within the protein is a valuable tool for structure-function investigations in membrane proteins, particularly in excitable membranes, where the membrane potential is responsible for regulating many physiological processes. Based on crystal structures, the electric field within the proteins may be calculated and the resulting predictions can now be tested by site-directed field measurements, as it was done in the case of the voltage sensor of the *Shaker* $K^+$ channel.

## Optically Detecting Membrane Potential in Genetically Specified Neurons

The electric field structure in voltage-gated ion channels is thus optimized for voltage-sensing. Together with the concerted action between different types of channels and the passive electrical properties of the neurons, this ensures the robust generation and propagation of action potentials in these cells. To understand the complex interactions in our central nervous system, it is essential to investigate the propagation of the signals in a complex network. Here, electrophysiological methods reach their limits very quickly due to the need for electrical access to each point of interest, a problem that optical methods do not share (Salzberg et al., 1977). Due to their scalability, they are highly advantageous. Optical detection is possible with high temporal and spatial resolution, and with fast enhanced charge-coupled device (ECCD) cameras becoming available with high quantum efficiency and low background noise, the optical signals from larger areas may be recorded. This has proven to be possible with $Ca^{++}$-dyes that have been used to record optical signals within a complex network (reviewed in Helmchen & Waters, 2002).

But in order to detect changes in the membrane potential directly, probes for the electric field are required. The fastest voltage-sensitive dyes are styryl dyes such as di-8-ANEPPS (Bedlack, Jr. et al., 1994;

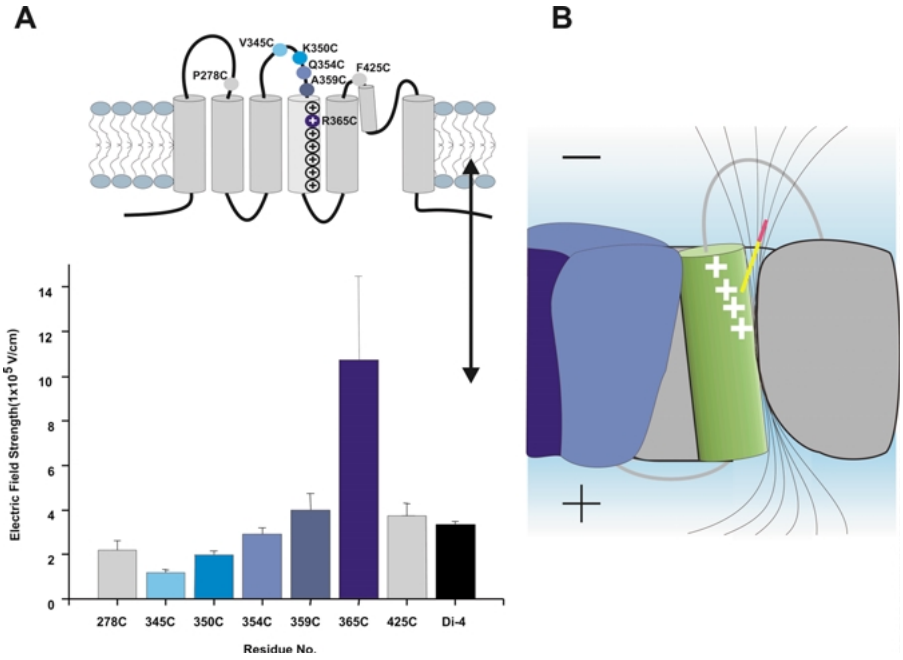


**Fig. 3.** Shape of electric field around S4. (*A*) The electric field strength increases along the S4 segment. The calibration was done using di-4-ANEPS in the oocyte membrane (*black*). (*B*) Schematic of the electric field lines around the S4. The field is compressed inside the water-filled crevices. The likely orientation of ANEPIA is indicated by the yellow rod with the chromophore displayed in red.

Zhang et al., 1998). Dyes of this type have been shown experimentally to respond in less than 2 μs using the squid giant axon (Salzberg, Obaid & Bezanilla, 1993) and voltage-dependent fluorescence changes up to 22% per 100 mV change in membrane potential have been reported (Rohr & Salzberg, 1994). But the largest fluorescence changes are obtained using Förster Resonance Energy Transfer (FRET), where translocation of donor or acceptor fluorophore are translated into fluorescence changes due to the distance-dependence of the energy transfer (Lakowicz, 1999). Gonzalez and Tsien (1995; 1997) designed an optical voltage sensor consisting of a membrane-bound fluorophore and an oxonol dye, which partitions into the membrane and distributes between the inner and the outer leaflet of the plasma membrane as a function of the membrane potential. With this system, fluorescence changes up to 34% per 100 mV were recorded but at the cost of a far slower response time than electrochromic dyes. Despite its slow kinetics, this combination has been employed successfully to monitor locomotor activity in single neurons in leech nerve cords (Cacciatore et al., 1999).

## The GFP Problem

When observing function in a neuronal network or tissue by optical means, there are many considerations that call for special characteristics of the probes. One of them is the penetration depth of the probe in the tissue. Very lipophilic dyes, such as di-8-ANEPPS or the fast oxonol (Gonzalez & Tsien, 1997) have a short diffusion length in the neuronal tissue, and are, therefore, not as useful as expected. More importantly, one wishes to target a specific population of cells, since only the neurons are electrically active, while the surrounding glial cells only add to the background fluorescence or contribute confounding optical signals (Konnerth et al., 1987). Furthermore, one would like to record signals from a selected subset of neurons so that one can assign the recorded signals to the cells they originated from and identify the nature of the circuit elements in the neuronal process. This has been achieved by injecting di-8-ANEPPS, or other impermeant probes into single neurons. However, in order to reach the goal of recording from a specified population of cells, it is necessary to encode the probe genetically. Fluorophores, such as GFP and its family members have previously been employed successfully to measure $Ca^{++}$-concentration, $Cl^{-}$-concentration and pH (Miesenbock, De Angelis & Rothman, 1998; Kuner & Augustine, 2000; Ng et al., 2002; Wang et al., 2003; Rogers et al., 2005). GFP variants could be engineered that are sensitive to $Cl^{-}$ (Kuner & Augustine, 2000) and pH (Miesenbock et al., 1998), and the pH-dependent pHlorin constructs have been applied to measure fusion of individual secretory granules and synaptic transmission in antennal lobe of *Drosophila* (Ng et al., 2002). With the aim of determining a functional map of the antennal lobe of *Drosophila* (Wang et al., 2003), a $Ca^{++}$-sensitive GFP was also constructed (Miyawaki et al., 1997; Nakai, Ohkura, and Imoto, 2001). In contrast to $Cl^{-}$ and pH, simple mutations of the GFP were insufficient to make it $Ca^{++}$-sensitive. Therefore, the N-terminus of GFP was fused to a myosin light chain fragment and its C-terminus to Calmodulin. Similarly, Romoser et al.

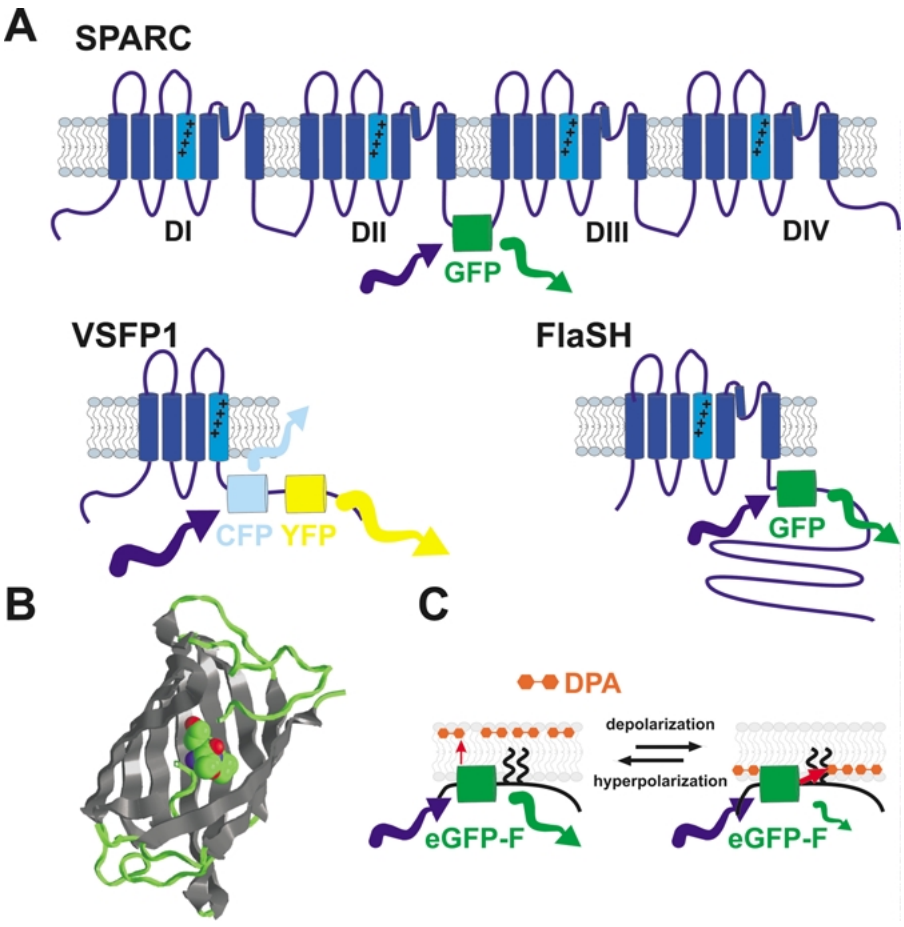


**Fig. 4.** Design of genetically encoded fluorescent voltage sensors. (*A*) Voltage sensors based on voltage-gated ion channels. SPARC consists of an rSKM1 channel with a GFP introduced in the linker between domains II and III. VSFP1 comprises the isolated voltage sensor of the $K_V2.1$ channel fused to a tandem of a CFP and YFP on the C-terminus. In FlaSH, a GFP or CFP is fused to the C-terminus of the S6 segment in the *Shaker* $K^+$ channel. (*B*) Structure of GFP. The fluorophore (shown spacefilling) is protected inside the beta-barrel structure surrounding it. Residues 1–47 were removed for clarity. (*C*) The hybrid voltage sensor (hVOS) consists of a GFP fused to a farnesylation and palmitoylation motif (*black*) and the absorber DPA (*orange*) that partitions into the membrane. Upon depolarization, the DPA translocates from the outer to the inner leaflet of the membrane so that excited states are transferred to DPA and the GFP fluorescence decreases.

(1997) made a FRET construct consisting of a bGFP and rGFP coupled by the calmodulin-binding domain of a myosin light chain kinase. Upon binding of $Ca^{++}$ these constructs change their conformation and alter the FRET efficiency between the attached fluorescent proteins. Brûlet and his coworkers designed a very elegant construct consisting of the $Ca^{++}$ concentration-dependent and bioluminescent Aequorin, fused to the C-terminus of GFP (Baubet et al., 2000). In this way, they overcame the low quantum yield of Aequorin. By fusing this construct to different proteins, they were able to target it to specific pre- and postsynaptic compartments (Rogers et al., 2005) and they recorded $Ca^{++}$ oscillations from these positions.

For the detection of membrane potential, GFP-based constructs have been designed by fusing the protein to a $K^+$ or $Na^+$ channel (Fig. 4*A*). Since conformational changes in voltage-gated ion channels are the result of voltage changes across the membrane, a coupled chromophore like GFP may detect the intra-protein movements that follow membrane potential changes. The first reporter protein called FlaSH was generated by inserting the GFP into the C-terminus of the S6 helix (Guerrero & Isacoff, 2001; Siegel & Isacoff, 1997). However, the fluorescence of this construct was governed by the kinetics of C-type inactivation so that the response time was relatively slow. The next generation of FlaSH proteins had a faster time constant (~10 ms), but still recovered very slowly after a detected event (Guerrero et al., 2002). The SPARC construct, where the GFP was inserted into a sodium channel in the linker between domains II and III, had much faster kinetics with response time constants down to 0.7 ms (Ataka & Pieribone, 2002). Another construct, VSFP1 was based on a truncated voltage sensor, to which a CFP (cyan) -YFP (yellow) pair was attached. Upon changes in the membrane potential the relative orientation between the two fluorophores was altered, modulating the FRET-efficiency from CFP to YFP (Sakai et al., 2001; Knopfel et al., 2003). These constructs used ion channels as voltage sensors but, as voltage-gated ion channels are optimized to respond to very small changes in the membrane potential, the dynamic range is reduced, which becomes particularly apparent for FlaSH and SPARC. Due to this property, on the other hand, these probes give an amplified response to a small signal crossing the threshold voltage. Although all these designs successfully recorded potential changes in model sys-

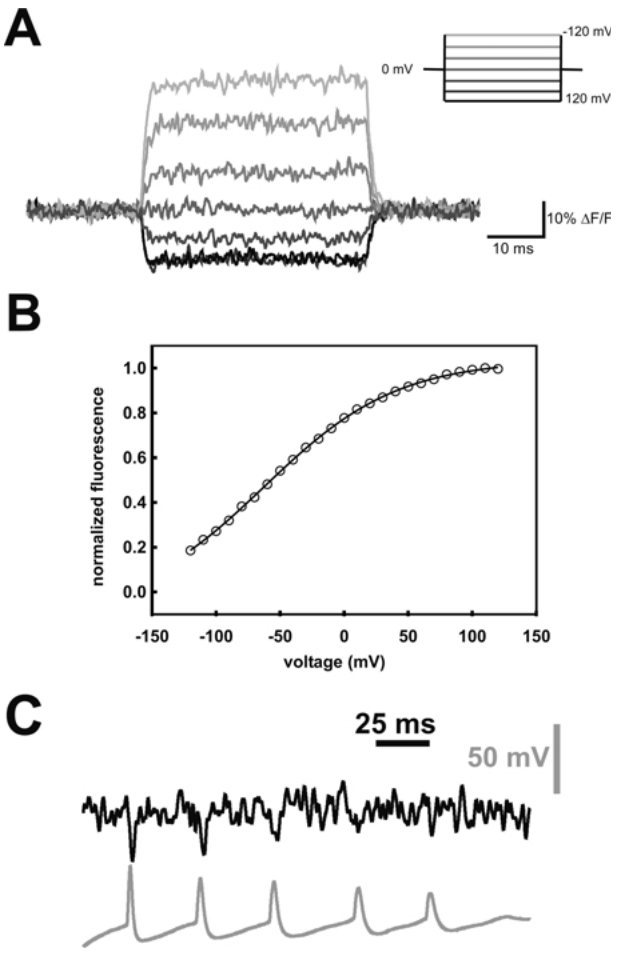


**Fig. 5.** Fluorescence response of hVOS. (*A*) Fluorescence response of hVOS expressed in HEK293 cells to square voltage pulses from −120 mV to +120 mV in steps of 40 mV. (*B*) Fluorescence-voltage relationship of hVOS in HEK293 cells. (*C*) Fluorescence detection (*black trace*) of a train of spontaneous action potentials (*grey trace*) in primary cultured neurons. (Modified and reproduced with permission by Nature Neuroscience from Figs. 1 and 6 of Chanda et al., 2005b).

tems, the fluorescence response was very small. As a consequence, in the more complex natural neuronal environment, the signals could not be detected. Roorda et al. (Roorda et al., 2004) attempted to circumvent this problem by using second harmonic generation (SHG) signals, which are sensitive to ordered phases, by aligning the GFP with an N- and a C-terminal anchor to the inner leaflet of the plasma membrane, but could not find a sufficient SHG signal.

In these constructs, the use of GFP as a voltage sensor is complicated by the protected position of the actual fluorophore inside a beta-barrel (Fig. 4*B*, Ormo et al., 1996). This configuration shields the fluorophore against parametric changes in the environment. Another problem is that the GFP cannot be placed "inside" the membrane, where the electric field changes occur, but is always located in the vicinity. As a consequence, the fluorophores require an additional sensor module.

## The Hybrid Approach

While the largest fluorescence changes are obtained using the FRET system from Gonzalez and Tsien (1997), the use of GFP is essential to specify the neurons of interest genetically. Therefore, the hybrid voltage sensor (hVOS) combines the beneficial properties of both systems (Chanda et al., 2005b). It uses a membrane-bound GFP to genetically encode the fluorescent donor, and pairs it with a synthetic compound, dipicrylamine (DPA), as a voltage-sensing acceptor. The coupling between the two compounds occurs via FRET (Fig. 4*C* and Fig. 6*A*).

### *The Components*

The genetic component was chosen to be an eGFP fused to the 20-aminoacid farnesylation sequence derived from c-Ha-Ras that provides a palmitoylation and farnesylation site. The mature protein is thus actively recruited to the inner leaflet of the plasma membrane (Jiang and Hunter, 1998). The GFP-compound, therefore, forms a passive "reporter tag", whose fluorescence is modulated by the actual sensor, the DPA. By choosing not to fuse the GFP to a membrane protein, we prevented large amounts of proteins from being sequestered within the ER and other intracellular membranes (Riven et al., 2003; Blunck et al., 2004) and we, thereby, reduced the background fluorescence to a minimum.

The functional component is a small non-fluorescent synthetic compound, DPA, that partitions into the membrane, where it can diffuse between the outer and inner leaflet (Fig. 4*C*). Since it is negatively charged, it distributes across the membrane in a voltage-dependent manner (Fernandez, Taylor & Bezanilla, 1983; Chanda et al., 2005a). At negative resting potentials, most of the DPA molecules stay at the outer leaflet. Upon depolarization of the membrane, the DPA translocates to the inner leaflet close to the GFP. Compared to oxonol, DPA is much less lipophilic than the fast moving variant of oxonol (Gonzalez & Tsien, 1997) and therefore diffuses with ease through more complex networks, which makes it applicable to, e.g., brain slices. Furthermore, as DPA is not fluorescent, partitioning into the membrane of cells surrounding the targeted neurons does not increase the background fluorescence. Still, the two components of this hybrid voltage-sensing system are coupled via FRET. Prerequisite for this process is that the acceptor absorbs in the range of donor

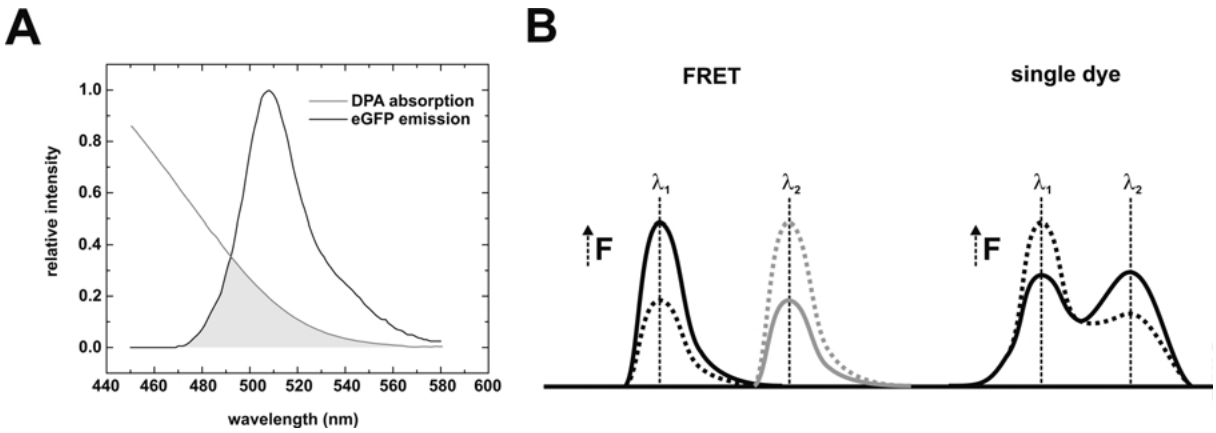


**Fig. 6.** FRET and ratiometric measurements. (*A*) Emission spectrum of eGFP and absorption spectrum of DPA. The shaded area indicates the overlap determining the $R_0$. Note that the DPA absorption spectrum is blue-shifted with respect to the eGFP emission. (*B*) Change of the spectra in FRET and ratiometric systems upon stimulus (change of energy transfer and $Ca^{++}$-concentration, respectively).

emission (*see* Fig. 6*A*). At the resting membrane potential, the DPA residing on the outer leaflet of the bilayer is at a distance $>40$ Å from the GFP, so only very little resonance energy transfer occurs (Fig. 4*C*, left). Upon depolarization, the DPA translocates to the inner leaflet, and thus comes into close proximity of the GFP. The resulting high transfer rate leads to a decrease in the donor emission intensity. The $R_0$, the distance between donor and acceptor at which 50% of all excited states are transferred to the acceptor, is 37 Å for this pair and therefore optimal for the thickness of the bilayer (30–50 Å).

### *Speed and Sensitivity*

The fluorescence change is dependent on the DPA concentration (for obvious geometric reasons) and reaches 34% per 100 mV at 6 μM DPA (Fig. 5*A*). Due to the low charge of DPA, the charge movement occurs over a large voltage range (−180 mV to +100 mV) (Fig. 5*B*). Since the voltage dependence is approximately linear in the range from −150 mV to +50 mV, the magnitude of the fluorescence change can be calibrated for direct measurement of the absolute membrane potential change. The time constant of the jump response is 500 μs, which means that it may be possible with this system to follow action potentials in neurons, which typically cover a voltage range from −70 mV to 40 mV and have durations $>1$ ms.

Using hVOS, we have successfully recorded trains of spontaneous action potentials from cultured primary neurons (Fig. 5*C*). This capability has not previously been realized using genetically targeted molecular indicators of membrane potential (potentiometric probes). Owing to the use of lower DPA concentrations (*see* below), the average magnitude of the action potential signals was 4.2% per 100 mV. But the use of hVOS is not restricted to neuronal tissues. In vivo expression of hVOS in mammalian skeletal muscle fibers targets the fluorophores exclusively to the T-tubule membranes (DiFranco et al., *unpublished results*). The detection of action potentials in muscle fibers with two-photon excitation resulted in a fluorescence spike of 5% ($\Delta F/F$) with a time constant of ~1 ms.

### The Capacitive Load Problem

For the recordings in the neuronal cells, the applied DPA concentration had to be reduced in order to prevent abolition of action potentials (Chanda et al., 2005b). The reason for this lies in the increased membrane capacity contributed by DPA. During the rising phase of the action potential, the influx of $Na^+$ supports the charging of the membrane capacity and thereby further depolarization and opening of $Na^+$ channels. Nevertheless, since DPA is actually negatively charged and translocates through the membrane, it increases the capacitive load on the membrane. As a consequence, the charging of the membrane is seen as a slowing down of the rising phase of the action potential and a decrease of the peak amplitude due to the repolarization by the potassium current[2]. A further increase

[2]During the onset of a membrane action potential, the current is carried mainly by the opening of the sodium channels ($I_{Na}$). Therefore, the change in membrane potential is approximately given by $dV/dt = -I_{Na}/C$, and since $I_{Na}$ remains approximately constant, an increase in $C$ reduces $dV/dt$ so that the transmembrane voltage develops more slowly.

of the capacitive load results in complete abolition of the action potential. This problem is not intrinsic to the hybrid system, but is true for all systems that sense the potential by charge translocation. Therefore, the voltage-gated ion channel-based systems also have the same problem. Each ion channel adds 12 $e_0$ to the membrane. In fact, for ion channels, the capacitive load problem is even more severe, since their voltage dependence is steeper. This means that the charges have to be moved over a smaller voltage range, within which the capacitive load has to be overcome. In contrast, electrochromic dyes, like di-8-ANEPPS, do not have this problem, since here the interaction of the electric field with the electronic states of the fluorophore lead to a shift in the fluorescence spectra, so the charges move through a very small fraction of the membrane field (the size of the chromophore).

It is important to realize that the hybrid approach allows for the substitution of the actual voltage-sensing component. For example, a combination of the membrane-coupled GFP (eGFP-F) with an electrochromic dye would improve the capacitive problem of hVOS. Nevertheless, many electrochromic dyes are very lipophilic, so that their diffusion length in tissues is limited. Another problem is that di-8-ANEPPS has a very broad absorption and emission spectrum, while the shifts in the spectra are relatively small. One can achieve large fractional changes in the fluorescence intensity by choosing the excitation wavelength and narrow emission filters in the steepest range of the spectra. For a combination with the eGFP-F, the tuning of the wavelength is very limited so that the fractional changes would become very small. Since all surrounding cells would be labeled with the electrochromic dye, one still would have to observe the changes in the donor emission, so that the signal could not be enhanced by using a narrow emission filter. One might wonder whether it is possible to excite the eGFP-F so that the electrochromic dye is excited exclusively by FRET in the targeted neurons. This is, in fact, a good possibility, which would work if there were very little direct excitation of the electrochromic dye (well separated spectra, 2-photon excitation). Another possibility is to use a non-fluorescent molecule that partitions into the membrane and exhibits the Stark effect; this molecule would have to be selected to have its absorption spectrum overlap with the emission of the GFP.

## Ratiometric Versus Single-Wavelength Detection

The hybrid approach we have presented here raises the question whether it is actually better to use a fluorophore or a pure absorber as an acceptor. As we mentioned earlier, the Förster theory does not require the acceptor to emit photons itself as long as the absorption spectrum overlaps with the donor's emission spectrum, i.e., as long as the excited state fits energetically with the acceptor states (Fig. 6*A*). Ratiometric measurements have many advantages, such as elimination of bleaching, variations in the excitation light and variations in scattering. By choosing the correct wavelength, one may even amplify the signal. Nevertheless, these advantages are true for a single dye system, like, for instance, $Ca^{++}$-indicators, where all fluorescence originates from the same population of fluorophores (Fig. 6*B*). For FRET systems, where donor and acceptor are spatially separated from each other and have distinct properties (bleaching, dependence on environment), those advantages are not necessarily valid (Chanda et al., 2005b)[3].

Fluctuations in the excitation intensity would influence all components of donor and acceptor fluorescence to the same degree, and are therefore well corrected by forming the ratio from donor and acceptor emission. Independent of this, it is advisable to use only very stable light sources. Sources using light-emitting diodes deliver particularly stable light intensities over tens of seconds (Rumyantsev et al., 2004; Salzberg et al., 2005). In cases where this is not possible, the excitation intensity may be recorded in a second channel for intensity correction.

In ratiometric measurements with a single fluorophore, the bleaching time course is also corrected, given that the background fluorescence is much smaller than the fluorescence signal. For FRET systems, this is no longer true. Most likely, the two fluorophores will have different bleaching time constants so that the ratio of donor and acceptor emission will be distorted. In fact, it is even more complicated since bleaching of acceptors will *increase* donor fluorescence. The intensities should therefore be carefully adjusted to minimize bleaching of both components. Synchronous changes in both recording channels — again under the assumption that the background fluorescence is low — are eliminated by forming the ratio of both intensities. These changes may be caused by a movement of the samples leading to altered scattering or by a change in the optical pathlength. This is also true for FRET measurements, as long as both partners are affected to the same degree, as would be the case for most "macroscopic" movements. Changes in the immediate environment of the fluorophores, on the other hand, leading to spectral shifts or changes in the quantum yield, would not be compensated. However, changes of this nature are very unlikely unless they are

[3]In supplementary note.

deliberately instigated, in which case they would be part of the signal.

It is generally thought that ratiometric measurements increase the signal-to-noise ratio (SNR). We have simulated FRET signals with different transfer efficiencies in a background-free system and investigated whether a spike-like signal would be easier to recognize in a ratiometric system as compared with a donor-only signal. In order to take the quantum nature of light into consideration, the noise was simulated by shot noise. The results of the simulations show that *under certain circumstances*, indeed, ratiometric measurements increased the SNR, which became very large under extreme conditions. This was always the case, provided the donor fluorescence signal increased during the spike. On the other hand, a decrease in the donor intensity led to a decreased SNR in ratiometric measurements. Interestingly, both effects are minimized for small signals, so that the SNR of donor emission measurement or ratiometric measurement for small signals are identical. The reason for the changes is mainly based on the non-linearity of the ratio and the fact that with extreme signals the acceptor (denominator) in a noiseless system becomes very small. The conclusion of these simulations is that the SNRs differ significantly between donor emission and ratiometric measurements only if the actual signals themselves are already large (Chanda et al., 2005b).

However, there are other considerations when comparing ratiometric to donor-only recordings. Ratiometric measurements require additional equipment, synchronization of both channels and eventually longer readout times for ECCD cameras. In addition, in the case of the hybrid approach the voltage-sensing acceptor would have to be fluorescent and that would increase background due to labeling of the surrounding cells, with the consequent decrease of the SNR. Even though only transfer from donors close to the acceptors should occur, most fluorophores have absorption at shorter wavelengths than their main absorption peak, so that the acceptor will be directly excited by the excitation light. Although this excitation efficiency may be small, the large number of acceptor fluorophores around the site of recording will make it very difficult to record the signal of interest. The use of a non-fluorescent acceptor (such as DPA) reduces the demands on the range of wavelength absorption characteristics of the acceptor since it only has to absorb in the donor emission region, leaving a potentially larger number of molecules that could be used. In the case of hVOS presented here, it allowed FRET from a rather unusual situation where the absorption spectrum of DPA is blue-shifted with respect to eGFP-F emission (Fig. 6*A*).

### Future Probes

The above considerations show that the perfect optical voltage sensor has not been found yet. The electrochromic dyes are not genetically encoded and show only small fractional changes, while all systems using charge to sense changes in the membrane potential harbor the intrinsic capacitive load problem. Here, the hybrid approach may point in the right direction, since its modular design allows for the combination of different beneficial compounds. Particularly, the fact that it is not necessary to have a fluorescent voltage-sensing acceptor increases the number and type of available molecules significantly. For example, it is possible to think of a combination of electrochromic dyes with eGFP-F, given that the dye absorbs in the appropriate region and has a long diffusion length. Also the GFP compound may be varied, as we have used a fluorescently labeled antibody in combination with DPA to detect potential changes (Chanda et al., 2005b). A perfect solution would, of course, be a purely genetically encoded probe that does not alter the intrinsic properties of the plasma membrane. In this case, the use of ion channels as the voltage sensors are the most likely candidates. In the membranes of neurons ion channels are present in high densities. If one succeeds in recruiting the intrinsic ion channels as voltage sensors — possibly in combination with another reporter protein — the charge translocation would not increase the capacitive load of the membrane over its basal level.

## Concluding Remarks

The techniques discussed here enable the optical recording of electric field changes, but on entirely different spatial scales. Di-1-ANEPIA gives information about the electric field distribution within a membrane protein and will be — in combination with electrophysiology and X-ray crystallography — an invaluable aid in resolving structure–function relations for membrane proteins whose function relies on membrane potential changes (e.g., channels and transporters, but *see* also Murata et al., 2005), but may also be useful for proteins that are involved in the electron transport chain or photosynthesis or even to map the influence of local electric field on the function of voltage-independent membrane proteins. The hybrid approach enables the optical observation of neuronal activity in a complex network (cf., Obaid et al., 2004). The approach of separating the genetically-encoded fluorescent reporter from the sensor module opens many new possibilities for other hybrid optical reporter systems. Not only may the components be optimized (distance dependence, faster probes), but the sensor may also be varied to

detect changes in other physiologically important parameters, e.g., $Ca^{++}$ or pH.

## Appendix

### Experimental Designs

#### Cut-open Oocyte Fluorescence

The measurements of the electric field within the voltage-gated ion channels require a fast voltage-clamp system and good signal to noise ratio. Therefore, all these experiments were done in the cut-open oocyte voltage-clamp configuration (Cha & Bezanilla, 1998). The cut-open design allows a very fast clamping ($\tau < 30$ μs) and therefore allows distinction between the electrochromic on and off signals (Fig. 2*C*) and the signal that follows the conformational changes and reorientation of the field ($\tau > 100$ μs). The electric field strength was determined from the slope of the fluorescence-voltage relationship (Asamoah et al., 2003). The slope delivers the $dF/dV$ of di-1-ANEPIA at the specific position. This value was calibrated to di-4-ANEPPS in the oocyte membrane with uniform potential gradient ($\Delta V/\Delta x$), so that an absolute value for the field strength could be estimated. The value constitutes a lower estimate of the actual value at that position because di-1-ANEPIA is constrained by the surrounding protein, so its dipole moment may not necessarily be aligned with the electric field.

#### Patch-Clamp Fluorometry from Cells

For fluorescence measurements from patch-clamped cells, a setup based on an inverted microscope was used (Blunck et al., 2004). Cells were transfected with eGFP-F and transferred into petri dishes with glass coverslip bottoms. Under steady perfusion with $O_2$-rich solution, the cells were patched in whole-cell configuration. Action potentials were stimulated and recorded in whole-cell current-clamp configuration. As excitation light source, blue light-emitting diodes (Lumileds) or a mercury lamp with stabilized power supply were used. The fluorescence emission was recorded using a cooled avalanche photodiode connected to a patch-clamp amplifier (Photomax 200 APD, Dagan Corp., Minneapolis, MN).

The main concern in all fluorescence measurements from cells is to minimize the background fluorescence. To this end, the excitation area was reduced to the region of interest; the reduction of this area in the limit becomes a diffraction-limited spot as in confocal spot detection. On the detector side, all fluorescence not originating from the region of interest was masked. Particularly in thicker tissue, as, for instance, brain slices or muscle fibers, two-photon excitation reduces the background even further (diFranco et al., *unpublished results*).

## References


Aggarwal, S.K., MacKinnon, R. 1996. Contribution of the S4 segment to gating charge in the Shaker $K^+$ channel. *Neuron* **16:**1169–1177

Ahern, C.A., Horn, R. 2005. Focused electric field across the voltage sensor of potassium channels. *Neuron* **48:**25–29

Asamoah, O.K., Wuskell, J.P., Loew, L.M., Bezanilla, F. 2003. A fluorometric approach to local electric field measurements in a voltage-gated ion channel. *Neuron* **37:**85–97

Ataka, K., Pieribone, V.A. 2002. A genetically targetable fluorescent probe of channel gating with rapid kinetics. *Biophys. J.* **82:**509–516

Baubet, V., Le Mouellic, H., Campbell, A.K., Lucas-Meunier, E., Fossier, P., Brulet, P. 2000. Chimeric green fluorescent protein-aequorin as bioluminescent $Ca^{2+}$ reporters at the single-cell level. *Proc. Natl. Acad. Sci. USA* **97:**7260–7265

Bedlack, R.S., Jr., Wei, M.D., Fox, S.H., Gross, E., Loew, L.M. 1994. Distinct electric potentials in soma and neurite membranes. *Neuron* **13:**1187–1193

Bezanilla, F. 2000. The voltage sensor in voltage-dependent ion channels. *Physiol. Rev.* **80:**555–592

Blunck, R., Starace, D.M., Correa, A.M., Bezanilla, F. 2004. Detecting rearrangements of shaker and NaChBac in real-time with fluorescence spectroscopy in patch-clamped mammalian cells. *Biophys. J.* **86:**3966–3980

Cacciatore, T.W., Brodfuehrer, P.D., Gonzalez, J.E., Jiang, T., Adams, S.R., Tsien, R.Y., Kristan, W.B., Jr., et al. 1999. Identification of neural circuits by imaging coherent electrical activity with FRET-based dyes. *Neuron* **23:**449–459

Cha, A., Bezanilla, F. 1997. Characterizing voltage-dependent conformational changes in the Shaker $K^+$ channel with fluorescence. *Neuron* **19:**1127–1140

Cha, A., Bezanilla, F. 1998. Structural implications of fluorescence quenching in the Shaker $K^+$ channel. *J. Gen. Physiol.* **112:**391–408

Cha, A., Snyder, G.E., Selvin, P.R., Bezanilla, F. 1999. Atomic scale movement of the voltage-sensing region in a potassium channel measured via spectroscopy. *Nature* **402:**809–813

Chanda, B., Asamoah, O.K., Blunck, R., Roux, B., Bezanilla, F. 2005a. Gating charge displacement in voltage-gated ion channels involves limited transmembrane movement. *Nature* **436:**852–856

Chanda, B., Bezanilla, F. 2002. Tracking voltage-dependent conformational changes in skeletal muscle sodium channel during activation. *J. Gen. Physiol.* **120:**629–645

Chanda, B., Blunck, R., Faria, L.C., Schweizer, F.E., Mody, I., Bezanilla, F. 2005b. A hybrid approach to measuring electrical activity in genetically specified neurons. *Nat. Neurosci.* **8:**1619–1626

Cohen, L.B., Salzberg, B.M. 1978. Optical measurement of membrane potential. *Rev. Physiol. Biochem. Pharmacol.* **83:**35–88

Fernandez, J.M., Taylor, R.E., Bezanilla, F. 1983. Induced capacitance in the squid giant axon. Lipophilic ion displacement currents. *J. Gen. Physiol.* **82:**331–346

Gonzalez, J.E., Tsien, R.Y. 1995. Voltage sensing by fluorescence resonance energy transfer in single cells. *Biophys. J.* **69:**1272–1280

Gonzalez, J.E., Tsien, R.Y. 1997. Improved indicators of cell membrane potential that use fluorescence resonance energy transfer. *Chem. Biol.* **4:**269–277

Guerrero, G., Isacoff, E.Y. 2001. Genetically encoded optical sensors of neuronal activity and cellular function. *Curr. Opin. Neurobiol.* **11:**601–607

Guerrero, G., Siegel, M.S., Roska, B., Loots, E., Isacoff, E.Y. 2002. Tuning FlaSh: Redesign of the dynamic voltage range, and color of the genetically encoded optical sensor of membrane potential. *Biophys. J.* **83:**3607–3618

Helmchen, F., Waters, J. 2002. $Ca^{2+}$ imaging in the mammalian brain *in vivo*. *Eur. J. Pharmacol.* **447:**119–129

Jiang, W., Hunter, T. 1998. Analysis of cell-cycle profiles in transfected cells using a membrane-targeted GFP. *Biotechniques* **24:**349–50,352, 354

Knopfel, T., Tomita, K., Shimazaki, R., Sakai, R. 2003. Optical recordings of membrane potential using genetically targeted voltage-sensitive fluorescent proteins. *Methods* **30:**42–48

Konnerth, A., Obaid, A.L., Salzberg, B.M. 1987. Optical recording of electrical activity from parallel fibres and other cell types in skate cerebellar slices *in vitro*. *J. Physiol.* **393:**681–702

Kuner, T., Augustine, G.J. 2000. A genetically encoded ratiometric indicator for chloride: capturing chloride transients in cultured hippocampal neurons. *Neuron* **27:**447–459

Lakowicz, J.R. 1999. Principles of Fluorescence Spectroscopy. 2nd Ed.

Mannuzzu, L.M., Moronne, M.M., Isacoff, E.Y. 1996. Direct physical measure of conformational rearrangement underlying potassium channel gating. *Science* **271:**213–216

Miesenbock, G., Angelis, D.A., Rothman, J.E. 1998. Visualizing secretion and synaptic transmission with pH-sensitive green fluorescent proteins. *Nature* **394:**192–195

Miyawaki, A., Llopis, J., Heim, R., McCaffery, J.M., Adams, J.A., Ikura, M., Tsien, R.Y. 1997. Fluorescent indicators for $Ca^{2+}$ based on green fluorescent proteins and calmodulin. *Nature* **388:**882–887

Murata, Y., Iwasaki, H., Sasaki, M., Inaba, K., Okamura, Y. 2005. Phosphoinositide phosphatase activity coupled to an intrinsic voltage sensor. *Nature* **435:**1239–1243

Nakai, J., Ohkura, M., Imoto, K. 2001. A high signal-to-noise $Ca^{2+}$ probe composed of a single green fluorescent protein. *Nat. Biotechnol.* **19:**137–141

Ng, M., Roorda, R.D., Lima, S.Q., Zemelman, B.V., Morcillo, P., Miesenbock, G. 2002. Transmission of olfactory information between three populations of neurons in the antennal lobe of the fly. *Neuron* **36:**463–474

Noda, M., Shimizu, S., Tanabe, T., Takai, T., Kayano, T., Ikeda, T., Takahashi, H., et al. 1984. Primary structure of *Electrophorus electricus* sodium channel deduced from cDNA sequences. *Nature* **312:**121–127

Obaid, A.L., Loew, L.M., Wuskell, J.P., Salzberg, B.M. 2004. Novel naphthylstyryl-pyridium potentiometric dyes offer advantages for neural network analysis. *J. Neurosci. Methods* **134:**179–190

Ormo, M., Cubitt, A.B., Kallio, K., Gross, L.A., Tsien, R.Y., Remington, S.J. 1996. Crystal structure of the *Aequorea victoria* green fluorescent protein. *Science* **273:**1392–1395

Posson, D.J., Ge, P., Miller, C., Bezanilla, F., Selvin, P.R. 2005. Small vertical movement of a $K^+$ channel voltage sensor measured with luminescence energy transfer. *Nature* **436:**848–851

Riven, I., Kalmanzon, E., Segev, L., Reuveny, E. 2003. Conformational rearrangements associated with the gating of the G protein-coupled potassium channel revealed by FRET microscopy. *Neuron* **38:**225–235

Rogers, Kelly L., Stinnakre, Jacques, Agulhon, Cendra, Jublot, Delphine, Shorte, Spencer L., Kremer, Eric J., Brulet, Philippe. 2005. Visualization of local $Ca^{2+}$ dynamics with genetically encoded bioluminescent reporters. Eur. J. Neurosci. 21:597–610

Rohr, S., Salzberg, B.M. 1994. Multiple site optical recording of transmembrane voltage (MSORTV) in patterned growth heart cell cultures: assessing electrical behavior, with microsecond resolution, on a cellular and subcellular scale. *Biophys. J.* **67:**1301–1315

Romoser, V.A., Hinkle, P.M., Persechini, A. 1997. Detection in living cells of $Ca^{2+}$ dependent changes in the fluorescence emission of an indicator composed of two green fluorescent protein variants linked by a calmodulin-binding sequence. A new class of fluorescent indicators. *J. Biol. Chem.* **272:**13270–13274

Roorda, R.D., Hohl, T.M., Toledo-Crow, R., Miesenbock, G. 2004. Video-rate nonlinear microscopy of neuronal membrane dynamics with genetically encoded probes. *J. Neurophysiol.* **92:**609–621

Rumyantsev, S.L., Shur, M.S., Bilenko, Y., Kosterin, P.V., Salzberg, B.M. 2004. Low frequency noise and long-term stability of noncoherent light sources. *J. Appl. Physics* **96:**966–969

Sakai, R., Repunte-Canonigo, V., Raj, C.D., Knopfel, T. 2001. Design and characterization of a DNA-encoded, voltage-sensitive fluorescent protein. *Eur. J. Neurosci.* **13:**2314–2318

Salzberg, B.M., Grinvald, A., Cohen, L.B., Davila, H.V., Ross, W.N. 1977. Optical recording of neuronal activity in an invertebrate central nervous system: simultaneous monitoring of several neurons. *J. Neurophysiol.* **40:**1281–1291

Salzberg, B.M., Kosterin, P.V., Muschol, M., Obaid, A.L., Rumyantsev, S.L., Bilenko, Y., Shur, M.S. 2005. An ultra-stable non-coherent light source for optical measurements in neuroscience and cell physiology. *J. Neurosci. Methods* **141:**165–169

Salzberg, B.M., Obaid, A.L., Bezanilla, F. 1993. Microsecond response of a voltage-sensitive merocyanine dye: fast voltage-clamp measurements on squid giant axon. *Jpn. J. Physiol.* **43:**S37–S41

Schonherr, R., Mannuzzu, L.M., Isacoff, E.Y., Heinemann, S.H. 2002. Conformational switch between slow and fast gating modes: allosteric regulation of voltage sensor mobility in the EAG $K^+$ channel. *Neuron* **35:**935–949

Seoh, S.A., Sigg, D., Papazian, D.M., Bezanilla, F. 1996. Voltage-sensing residues in the S2 and S4 segments of the Shaker $K^+$ channel. *Neuron* **16:**1159–1167

Siegel, M.S., Isacoff, E.Y. 1997. A genetically encoded optical probe of membrane voltage. *Neuron* **19:**735–741

Starace, D.M., Bezanilla, D.M. F 2001. Histidine scanning mutagenesis of basic residues of the S4 segment of the shaker $K^+$ channel. *J. Gen. Physiol.* **117:**469–490

Starace, D.M., Bezanilla, F. 2004. A proton pore in a potassium channel voltage sensor reveals a focused electric field. *Nature* **427:**548–553

Wang, J.W., Wong, A.M., Flores, J., Vosshall, L.B., Axel, R. 2003. Two-photon calcium imaging reveals an odor-evoked map of activity in the fly brain. *Cell* **112:**271–282

Zhang, J., Davidson, R.M., Wei, M.D., Loew, L.M. 1998. Membrane electric properties by combined patch clamp and fluorescence ratio imaging in single neurons. *Biophys. J.* **74:**48–53